Article

Discovery Medicine 2026; 38(207): 1131–1147
https://doi.org/10.24976/Discov.Med.202638207.91

CYP26A1 as a New Prognostic Biomarker With Immune Infiltration in Thyroid Cancer

Tingting Cui[1,*], Ying Zhang[2], Weida Liu[1], Danzhen Zhang[2], Haiying Gong[3]

[1]Department of Ultrasound, Taizhou Traditional Chinese Medicine Hospital, 318000 Taizhou, Zhejiang, China
[2]Medical Affairs Department, Taizhou Traditional Chinese Medicine Hospital, 318000 Taizhou, Zhejiang, China
[3]Department of Ultrasound, Yiwu Traditional Chinese Medicine Hospital, 322000 Yiwu, Zhejiang, China
*Correspondence: cuitingting0708@163.com (Tingting Cui)
Submitted: 6 January 2026 Revised: 27 February 2026 Accepted: 20 March 2026 Published: 20 April 2026

Background: Specific biomarkers for the diagnosis, treatment, and prognostication of thyroid cancer (THCA), the most common tumor in the endocrine system, are still lacking. *CYP26A1* is overexpressed in some cancers and exerts pro-tumor effects. However, its role in THCA development has not been established. Therefore, this study aims to comprehensively investigate the potential role of *CYP26A1* in THCA tumorigenesis and immune infiltration, as well as its clinical prognostic value.

Methods: Data from 510 THCA patients with complete progression-free interval (PFI) and tumor staging information were obtained from the Cancer Genome Atlas. Differentially expressed genes associated with high/low *CYP26A1* expression were identified and evaluated by Gene Ontology (GO) and Kyoto Encyclopedia of Genes and Genomes (KEGG) enrichment analysis, gene set enrichment analysis (GSEA), protein–protein interaction network construction, and miRNA-mRNA interaction network construction. Single-sample GSEA (ssGSEA) was performed to evaluate correlations between *CYP26A1* expression and immune cell infiltration. Associations between clinical pathological characteristics and the expression of *CYP26A1* were analyzed. Finally, the correlations between *CYP26A1* and the hub gene expression were evaluated, along with their relationships with sensitivity to chemotherapeutic drugs and small-molecule compounds.

Results: *CYP26A1* expression was higher in THCA than in paired para-cancerous tissues ($p < 0.001$). Genes associated with high *CYP26A1* expression in THCA were enriched in pathways related to the endoplasmic reticulum lumen, P53 signaling, cytokine receptor binding, and apoptosis signaling. *CYP26A1* expression was positively correlated with the abundance of various immune cells (T cells, B cells, CD8 T cells, cytotoxic cells, neutrophils, and Th1 cells). High *CYP26A1* expression was related to the PFI, T stage, cervical lymph node metastasis, and extra-glandular invasion ($p < 0.05$).

Conclusion: High *CYP26A1* expression is associated with THCA development and has prognostic value, suggesting its potential as a therapeutic target.

Keywords: *CYP26A1*; thyroid carcinoma; the Cancer Genome Atlas; diagnostic marker; prognostic marker

Introduction

Thyroid cancer (THCA), a common malignant tumor of the head and neck, constitutes 1%–2% of all human cancers, with incidence increasing annually [1]. THCA encompasses several histological types and subtypes presenting different cellular origins, characteristics and prognoses [2]; among these, the most common differentiated type is papillary thyroid carcinoma, followed by follicular thyroid carcinoma [3]. THCA is regarded as a low-grade cancer, with a recurrence rate of up to 30% and an early regional lymph node metastasis rate of 15% to 80% [4]. For patients with THCA, tumor capsule invasion and extra-glandular involvement, together with vascular invasion and distant metastasis, are strongly correlated with an unfavorable clinical prognosis [5]. Therefore, identifying the underlying biomarkers and pathological mechanisms of THCA, along with developing methods for the early and effective diagnosis and treatment, is crucial for early detection, tumor staging, prognosis evaluation, and drug development.

At present, the precise diagnosis of THCA remains a clinical challenge; however, many studies have found that abnormally expressed molecular biomarkers can be leveraged to aid diagnosis and inform treatment strategies. Although *BRAF V600E* [6] has been suggested to contribute to the diagnosis and risk assessment of THCA, its application is limited by a high false-negative rate. There is also growing evidence that long noncoding RNAs [7,8] are implicated in the occurrence and development of THCA via regulating related pathways or axes. In addition, miRNAs [9,10] participate in the occurrence, development, proliferation, invasion, and glycolysis of papillary thyroid carcinoma, and can serve as biomarkers to facilitate diagnosis, monitor recurrence, and determine prognosis. Owing to the widespread use of chip technology, a number of biomarkers for THCA diagnosis and prognosis have been

reported, such as *SEZ6L2* [11], *ANGPTL1* [12], *LRRK2* [13], and *ANXA10* [14]. Historically, *CYP26A1* was first cloned in zebrafish [15] and mainly functions in the regulation of retinoic acid (RA) levels in the human body. RA is a derivative of vitamin A, which is an indispensable factor for normal development and is essential in immune function, cell proliferation, differentiation, maturation, and apoptosis. Early research has established a plausible link between vitamin A deficiency and cancer [16]. Subsequently, increasing evidence has revealed that RA metabolic activity and *CYP26A1* levels are elevated in a variety of cancer types [17,18]. *CYP26A1* overexpression has also been observed in several cancers (breast cancer [19], cervical cancer, and pancreatic cancer [20]). However, the role and mechanism of *CYP26A1* in THCA remain unclear.

In this study, we probed into the relationship between *CYP26A1* and THCA. Using RNA-sequencing (RNA-seq) and clinical data for THCA retrieved from the Cancer Genome Atlas (TCGA) database, we explored the potential significance of *CYP26A1* in THCA occurrence and prognosis. Then, we observed *CYP26A1* overexpression in THCA and investigated its potential functions. Moreover, correlation analyses of *CYP26A1* levels with several clinical pathological features and prognosis were conducted. Molecular interaction network analysis and immune infiltration correlation analysis were performed to validate the biological significance of *CYP26A1*. Generally, our results demonstrated that *CYP26A1* is involved in the mechanisms underlying THCA and acts as a candidate diagnostic and prognostic biomarker.

Materials and Methods

Data Acquisition and Correlation Analysis

The sequencing count data from 510 THCA patients' tissues and 58 partially matched para-cancer tissues were downloaded from TCGA (https://portal.gdc.cancer.gov/) [21], and clinical data were obtained from the UCSC Xena (http://genome.ucsc.edu) website [22]. By integrating clinical and sequencing data, 510 THCA samples with complete progression-free interval (PFI) data and tumor stage information were included. To enable comparisons among samples, RNA-sequencing data were normalized to the fragments per kilobase per million (FPKM) format. According to the human genome annotation data, the genes were classified into protein-coding genes and long noncoding RNAs, and analyses were focused on protein-coding genes. In addition, FPKM datasets from TCGA and GTEx [23] were processed using the Toil pipeline via the UCSC-Xena platform to obtain the expression profiles of 33 TCGA cancer types and 31 GTEx normal tissues. This combined dataset was subsequently used for a pan-cancer gene expression analysis.

Differential Gene Expression and Functional Enrichment Analyses

Samples were divided into a low-expression group and a high-expression group using the median level of *CYP26A1* in THCA as a threshold. DESeq2 was used for a differential analysis of count data for THCA, and genes with $|\log_2(FC)| > 1$ and $p.adj < 0.05$ were identified as differentially expressed genes (DEGs).

Functional enrichment was performed across three categories: biological process, molecular function, and cellular component using Gene Ontology (GO) [24]. GO and KEGG pathway enrichment analyses of DEGs were carried out using the clusterProfiler R package [25]. A cutoff value of false discovery rate (FDR) <0.05 indicated significance, and the entry screening criteria were $p.adj$ value < 0.05 and q.value < 0.05. Corrected p-values were obtained using the Benjamini–Hochberg method [26].

A Gene Set Enrichment Analysis (GSEA) was performed to assess enrichment for a predefined set of genes related to a phenotype using the clusterProfiler package [27]. The parameters used in the GSEA were as follows: starting seed: 2020, number of calculations: 1000, and gene set size filter: >10 genes. The gene number was 500, and corrected p-values were obtained using the Benjamini–Hochberg method. The reference gene set was h.all.v7.1.symbols file, and the screening criteria for significant enrichment were $p < 0.05$, with FDR <0.20.

Protein–Protein Interaction Network Construction

The STRING database [28] included information on 2031 species, 9.6 million proteins, and 1.38 million protein-protein interactions (PPIs), integrating data from experimental studies, text-mined results for PubMed abstracts, other databases, and bioinformatics predictions. PPI networks for DEGs were constructed utilizing the STRING database. Results were visualized using Cytoscape (version 3.10.4, Cytoscape Consortium, Seattle, WA, USA) [29]. The CytoHubba plugin [30] was applied to analyze hub genes in the PPI network and to obtain the maximum correlation criterion (MCC) values for each node, ultimately highlighting the top 14 key genes.

Hub-miRNA Network Construction

Interactions between miRNAs and target genes were evaluated.

The miRTarBase database [31] included more than 8500 microRNA-mRNA targeting relationships (MTI, MicroRNA-Target Interactions) with supporting experimental evidence. However, with the addition of the newly released CLIP-seq dataset, the MTI collection in the new miRTarBase exceeds 500,000. By improving natural language processing technology, more target pairs, network functions, and annotation information were collected. In this study, the predicted miRNAs that bind to the hub genes were identified using the miRTarBase 2020

Table 1. Characteristics of THCA patients in the TCGA datasets.

Characteristic	Low expression of *CYP26A1*	High expression of *CYP26A1*	χ^2/Z	*p*
n	255	255		
T stage, n (%)			19.433	<0.001
T1	69 (27.1%)	74 (29.2%)		
T2	102 (40.0%)	65 (25.7%)		
T3	80 (31.4%)	95 (37.5%)		
T4	4 (1.6%)	19 (7.5%)		
N stage, n (%)			3.827	0.050
N0	121 (54.5%)	108 (45.4%)		
N1	101 (45.5%)	130 (54.6%)		
M stage, n (%)			0.091	0.763
M0	128 (96.2%)	158 (97.5%)		
M1	5 (3.8%)	4 (2.5%)		
Pathologic stage, n (%)			22.632	<0.001
Stage I	154 (60.4%)	132 (52.2%)		
Stage II	37 (14.5%)	15 (5.9%)		
Stage III	46 (18.0%)	67 (26.5%)		
Stage IV	18 (7.1%)	39 (15.4%)		
Gender, n (%)			0.089	0.765
Female	184 (72.2%)	187 (73.3%)		
Male	71 (27.8%)	68 (26.7%)		
Extrathyroidal extension, n (%)			16.180	<0.001
No	189 (77.1%)	149 (60.3%)		
Yes	56 (22.9%)	98 (39.7%)		
Race, n (%)			0.793	0.673
Asian	21 (10.9%)	30 (13.6%)		
Black or African American	12 (6.2%)	15 (6.8%)		
White	160 (82.9%)	176 (79.6%)		
Age, median (IQR)	45 (34, 58)	49 (36, 58.5)	–1.674	0.094

THCA, thyroid cancer; TCGA, the Cancer Genome Atlas; IQR, interquartile range. Some categories have missing clinical data; only cases with complete data were included in the final analysis.

(https://mirtarbase.cuhk.edu.cn/) database. The Starbase database (https://rna.sysu.edu.cn/encori/index.php) [32] included mRNA targets based on experimental data, including high-throughput CLIP-Seq, providing various interfaces for analyses. The database comprised rich miRNA-ncRNA, miRNA-mRNA, RBP-RNA, and RNA-RNA data.

Analysis of Clinical Features

The influence of *CYP26A1* gene expression and clinical pathological characteristics on patient prognosis was evaluated, especially relationships between CYP26A1 expression and various clinicopathological characteristics by logistic regression, and between CYP26A1 expression and PFI by Cox proportional hazards regression.

Assessment of the Tumor Microenvironment

Quantification of the relative abundance of each immune cell was achieved by a single-sample gene-set enrichment analysis (ssGSEA). Markers for each infiltrating immune cell type (e.g., activated dendritic cells, activated CD8 T cells, natural killer T cells, macrophages, and regulatory T cells) were evaluated, with the relative abundance represented by enrichment scores calculated from the ssGSEA [33]. The relationships between immune cells and hub gene expression levels were visualized using the ggplot2 package.

Drug Sensitivity Analysis

mRNA expression profiles and drug activity data for *CYP26A1* were acquired from the CellMiner database (https://discover.nci.nih.gov/cellminer/) [34]. Data on drug responses for 22,379 genes, 360 microRNAs, and 20,503 compounds were available on the CellMiner website. Correlations between *CYP26A1* gene expression and compound sensitivity were evaluated by a Pearson correlation analysis. $p < 0.05$ indicated a statistically significant relationship. The database was utilized to visualize interactions between hub genes and small-molecule drugs.

Statistical Analysis

All statistical analyses were implemented using the R software (Version 4.0.5, R Foundation for Statistical Com-

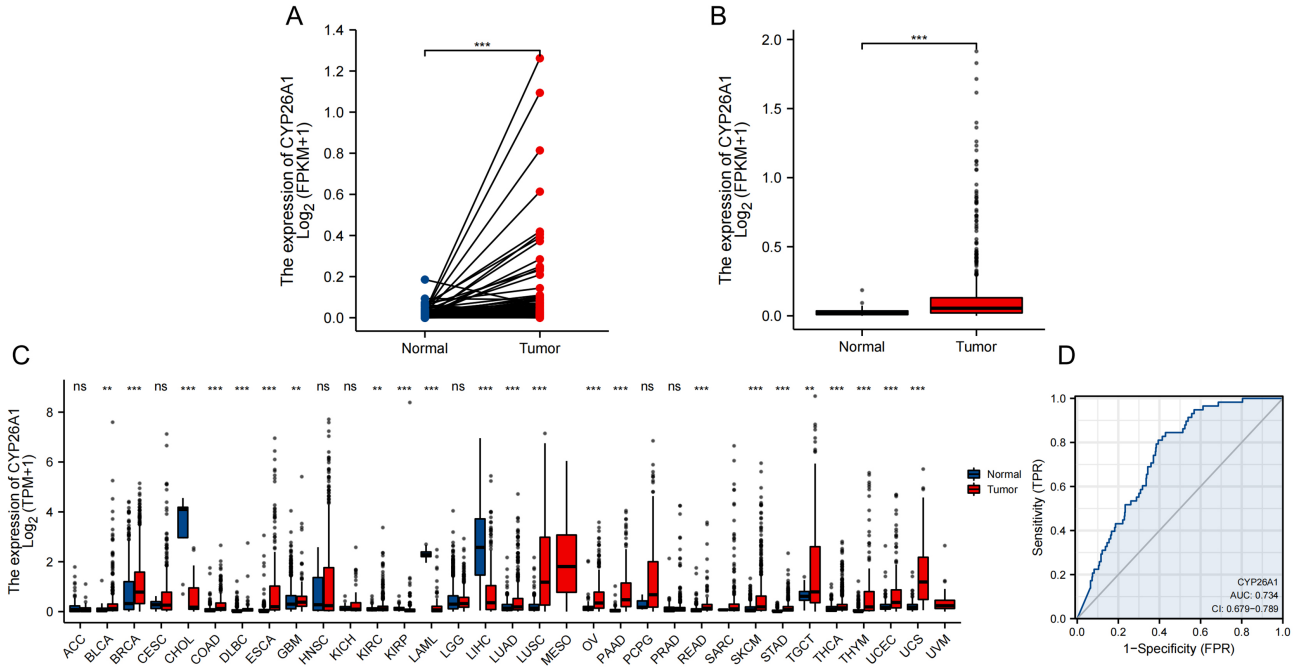

Fig. 1. *CYP26A1* expression was higher in THCA tissues and pan-carcinoma tissues than in control tissues. (A) *CYP26A1* expression in paired THCA and para-cancer tissues. (B) *CYP26A1* expression in unpaired THCA and para-cancer tissues. (C) Analysis of unpaired pan-carcinoma *CYP26A1*. (D) ROC curve of CYP26A1 for distinguishing THCA tissues from para-cancer tissues. $^{**}p < 0.01$, $^{***}p < 0.001$, ns, not significant. THCA, thyroid cancer; ROC, receiver operating characteristic.

puting, Vienna, Austria). Correlations were evaluated using Spearman's rank correlation coefficients. Continuous variables were presented as median (interquartile range, IQR). For group comparisons, we applied the Wilcoxon rank sum tests or the Wilcoxon signed rank tests for two groups and the Kruskal-Wallis test for three or more groups. PFI was compared using a Kaplan–Meier analysis and log-rank test. Unless otherwise stated, a $p < 0.05$ was the threshold for statistical significance.

Results

CYP26A1 Was Highly Expressed in THCA Tissues

In total, 510 THCA patients with complete PFI data and tumor staging information were analyzed (Table 1). A Wilcoxon signed rank test data showed that *CYP26A1* level was higher in THCA tissues than in paired para-cancer tissues ($p < 0.001$) (Fig. 1A). A comparison of unpaired THCA tissues and para-cancerous tissues using the Mann–Whitney U test (Wilcoxon rank sum test) revealed *CYP26A1* expression was higher in tumors than in adjacent normal tissues ($p < 0.001$) (Fig. 1B). In a pan-cancer analysis, *CYP26A1* expression was elevated in most malignant tumors (Fig. 1C). Therefore, *CYP26A1* has predictive value in distinguishing between THCA Tumor and Normal groups (AUC = 0.734, 95% CI = 0.679–0.789) (Fig. 1D).

Differential Expression and Functional Enrichment Analyses of CYP26A1

To unravel the possible mechanisms of *CYP26A1*, its biological characteristics, and related pathways in THCA, a low-expression group (0%–50%) and a high-expression group (50%–100%) were established according to the *CYP26A1* level in THCA. Using DESeq2 and threshold values of $|\log_2(FC)| > 1$ and $p.adj < 0.05$, 794 DEGs were identified. At this threshold, there were 685 highly expressed genes (positive logFC) and 109 lowly expressed genes (negative logFC) in the high group, as visualized using a volcano map (Fig. 2A).

We performed functional enrichment analysis on the DEGs using the GO and KEGG databases (Fig. 2 and Tables 2,3). A pathway enrichment analysis revealed that DEGs participated in type I diabetes mellitus, intestinal immune network for IgA production, hematopoietic cell lineage, viral protein interaction with cytokine and cytokine receptor, cytokine-cytokine receptor interaction, and other KEGG pathways (Fig. 2B,C and Table 3). We also detected enrichment for cell matrix components (collagen trimer, endoplasmic reticulum lumen, external side of plasma membrane, and collagen-containing extracellular matrix) (Fig. 2D,E), as well as molecular functions (extracellular matrix structural constituent, cytokine activity, chemokine activity, cytokine receptor binging, and receptor ligand activity) (Fig. 2D,E) (Table 2).

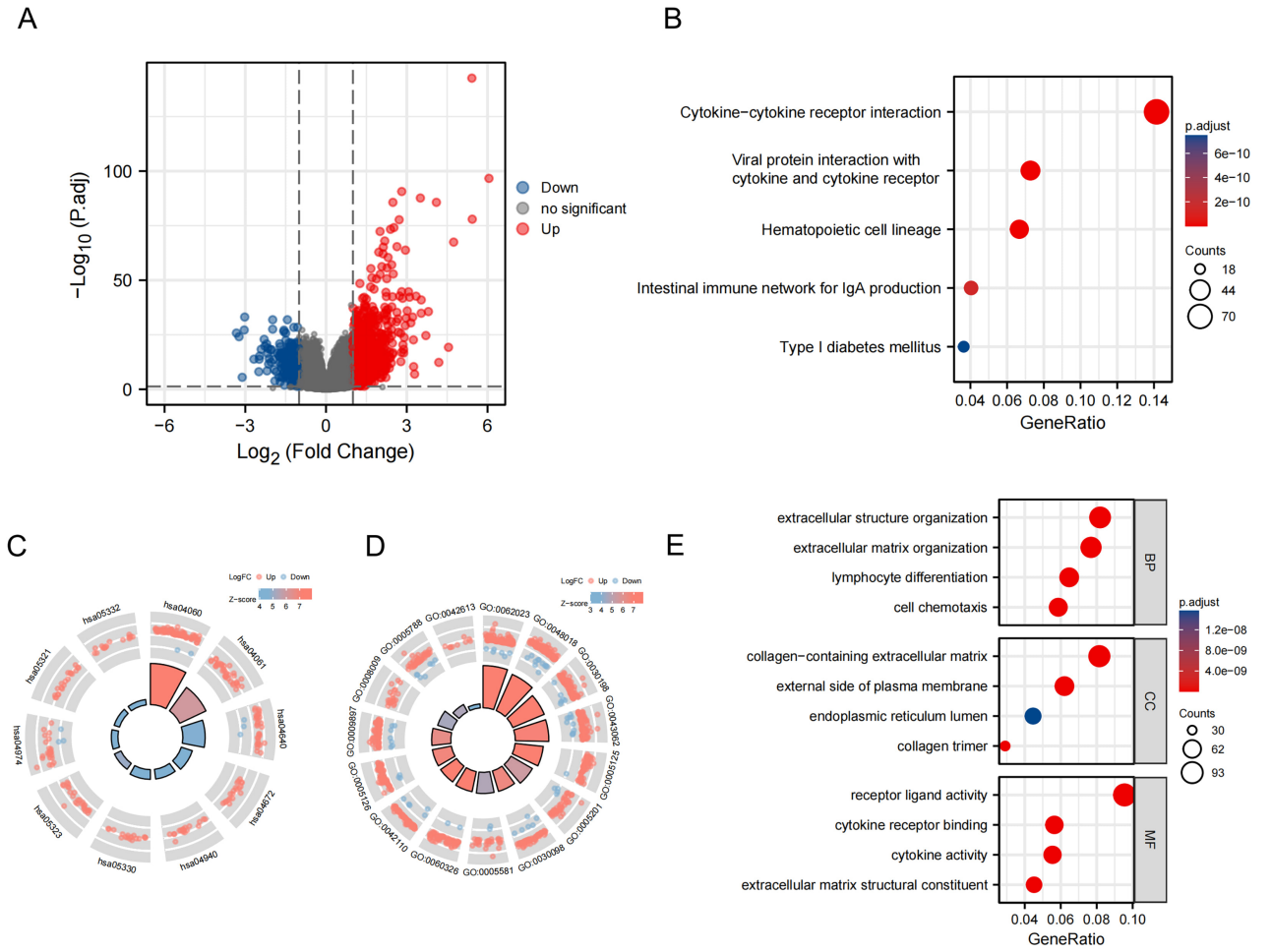

Fig. 2. Single gene difference analysis and functional enrichment analysis of *CYP26A1*. (A) Volcano map of differential mRNA analysis associated with CYP26A1 (x-coordinate = $\log_2$ FoldChange, y-coordinate = $-\log_{10}$ (Adjust *p*-value), red nodes = up-regulated differentially expressed genes (DEGs), blue nodes = down-regulated DEGs, and black nodes = genes insignificantly differentially expressed). (B) KEGG pathway enrichment analysis (x-coordinate = gene ratio, y-coordinate = pathway name, node size = the number of genes in the pathway, and node color = $-\log_{10}$ (*p*-value)). (C) The first ten items of KEGG analysis (node colors = gene expression levels, red = up-regulated genes, and blue = down-regulated genes; quadrilateral color representing Z-score of GO terms, blue = negative Z-score more likely inhibited in the corresponding pathway; red = positive Z-score more likely activated in the corresponding pathway). (D) Chord plot showing the GO terms (node colors = gene expression levels, red = up-regulated genes, and blue = down-regulated genes; the quadrilateral color representing the Z-score of GO terms, blue = negative Z-score more likely suppressed in corresponding GO terms, and red = positive Z-score more likely activated in corresponding GO terms). (E) Enrichment analysis of GO function (x-coordinate = Gene ratio, y-coordinate = –log(*p.* adjust); color of the bar chart representing GO terms (red: activation; blue: suppression). KEGG, Kyoto Encyclopedia of Genes and Genomes; GO, Gene Ontology.

To confirm the functions of DEGs associated with *CYP26A1* gene expression differences in THCA, a GSEA was performed. Fig. 3A shows an overview of the top 5 most significantly upregulated pathways. Among all significantly enriched pathways, we further focused on those most relevant to THCA tumorigenesis and progression, including the KRAS, P53 and apoptotic signaling pathways (Fig. 3A–E and Table 4).

PPI and Gene-miRNA Regulatory Network Construction

Interactions among proteins encoded by DEGs were assessed with STRING and visualized using a PPI network. Cytoscape was used to evaluate the network, in which node shapes and sizes were proportional to the extent of differences. In the network, genes in the treatment group were color-coded: blue for downregulated and red for upregulated (Fig. 4A). CytoHubba plug-in was used to identify the first 20 hub genes based on the MCC, where a darker color indicated a higher score, with the top 14 scores corre-

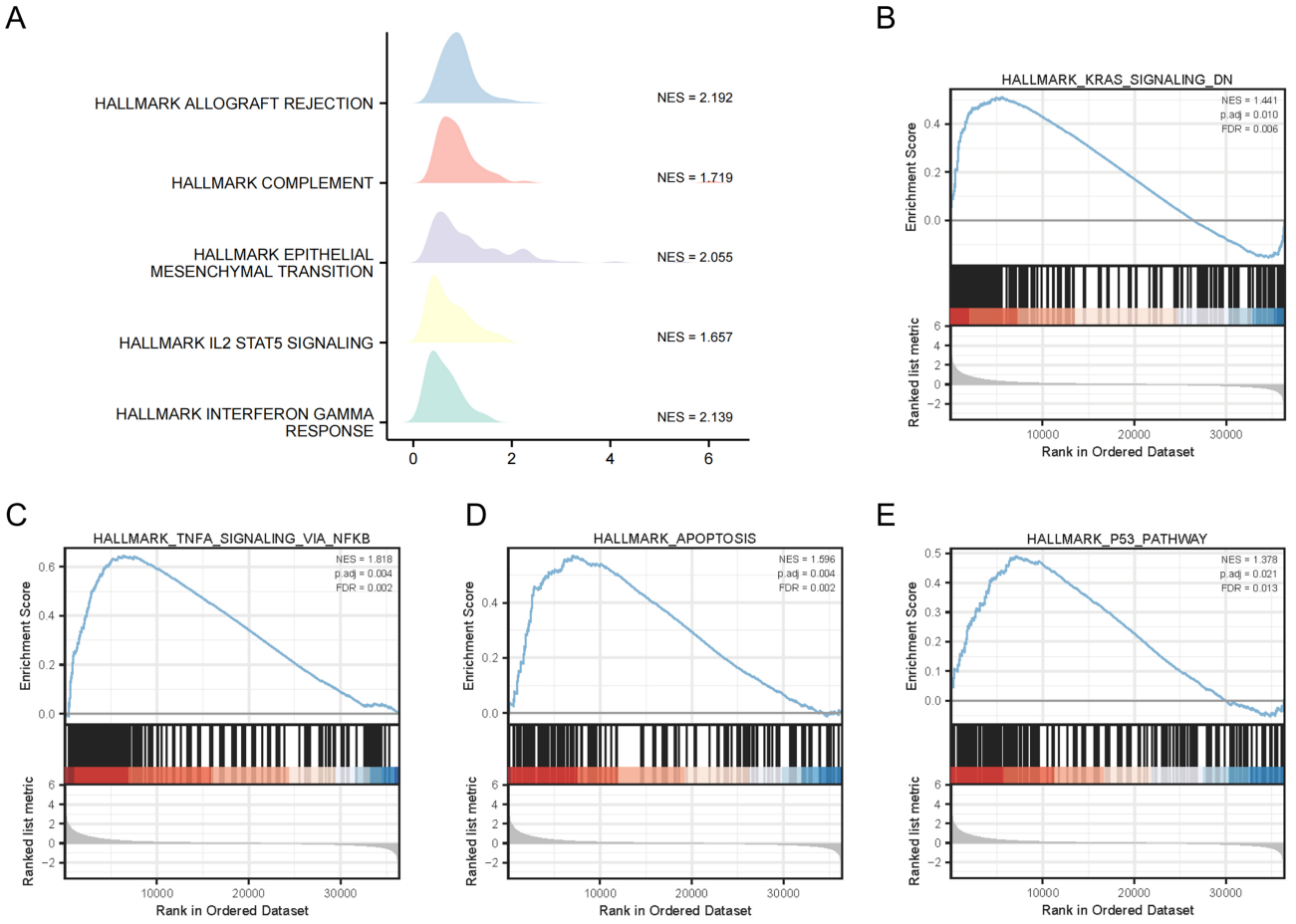

Fig. 3. GSEA enrichment analysis of differential genes. (A) Five main biological characteristics analyzed using GSEA. (B–E) Individual GSEA enrichment plots for pathways relevant to THCA tumorigenesis and progression, including KRAS signaling (B), TNFA signaling via NFKB (C), apoptosis (D), and P53 signaling (E). GSEA, gene set enrichment analysis; KRAS, kirsten rat sarcoma viral oncogene homolog; TNFA, tumor necrosis factor alpha; NFKB, nuclear factor kappa-light-chain-enhancer of activated B cells.

sponding to key genes (Fig. 4B). In addition, we obtained significant co-expression of hub genes with *CYP26A1*, as visualized using a heat map (Fig. 4C).

An mRNA–miRNA network was plotted with DEGs, containing 5 mRNAs and 557 miRNAs (Fig. 5). *COL1A2* was regulated by 145 miRNAs, *COL1A1* was regulated by 273 miRNAs, *VCAN* by miRNA, *CDH11* by 43 miRNAs, and *LUM* by 68 miRNAs (Fig. 5).

Immune Invasion Analysis

To evaluate relationships between *CYP26A1* expression and the degree of immune cell invasion, we employed a ssGSEA. Each type of invading immune cell was labeled, and clear differences in the abundance of most invading immune cells were detected between the two sets (Fig. 6A). In addition, *CYP26A1* expression was positively correlated to the abundance of various immune cells (T cells, B cells, CD8 T cells, cytotoxic cells, neutrophils, and Th1 cells) (Fig. 6B–G). These results suggest the interplay of *CYP26A1* and immune cell infiltration in THCA development and progression.

High CYP26A1 Expression Was Pertinent to the Pathological Features of Invasive Tumors

Influences of *CYP26A1* gene expressions on clinical pathological characteristics were clarified to determine its prognostic value. Analysis based on the PFI revealed that higher *CYP26A1* levels in THCA tissues were significantly associated with a poorer prognosis (Fig. 7A). In terms of T staging in THCA, high *CYP26A1* expression was related to a worse stage; for example, gene expression levels were remarkably higher in patients at T4 than in those at T1, T2 and T3, and also higher in T3 than in T2 (Fig. 7B, $p < 0.05$). We also found higher *CYP26A1* expression levels in patients with lymph metastasis (N1 stage), extrinsic thyroid invasion, or R1 resection (Fig. 7C–F, $p < 0.01$). In addition, a logistic regression analysis of relationships between clinicopathological characteristics and *CYP26A1* gene expression (classified as high or low) showed that the extrathyroidal extension and T staging were correlated with high *CYP26A1* gene expression ($p < 0.01$) (Table 5).

Table 2. GO enrichment analysis.

ONTOLOGY	ID	Description	GeneRatio	BgRatio	*p* value	*p*.adjust	q.value
BP	GO:0030198	extracellular matrix organization	76/989	368/18,670	3.78×10^{-25}	1.90×10^{-21}	1.45×10^{-21}
BP	GO:0043062	extracellular structure organization	81/989	422/18,670	1.58×10^{-24}	3.96×10^{-21}	3.02×10^{-21}
BP	GO:0030098	lymphocyte differentiation	64/989	353/18,670	2.86×10^{-18}	4.79×10^{-15}	3.65×10^{-15}
BP	GO:0060326	cell chemotaxis	58/989	304/18,670	9.80×10^{-18}	1.23×10^{-14}	9.39×10^{-15}
BP	GO:0042110	T cell activation	73/989	464/18,670	4.09×10^{-17}	4.10×10^{-14}	3.13×10^{-14}
CC	GO:0062023	collagen-containing extracellular matrix	84/1031	406/19,717	4.14×10^{-28}	1.90×10^{-25}	1.53×10^{-25}
CC	GO:0005581	collagen trimer	30/1031	87/19,717	2.63×10^{-17}	6.03×10^{-15}	4.87×10^{-15}
CC	GO:0009897	external side of plasma membrane	64/1031	393/19,717	3.95×10^{-16}	6.04×10^{-14}	4.87×10^{-14}
CC	GO:0005788	endoplasmic reticulum lumen	46/1031	309/19,717	1.37×10^{-10}	1.57×10^{-8}	1.27×10^{-8}
CC	GO:0042613	MHC class II protein complex	9/1031	16/19,717	2.32×10^{-8}	2.12×10^{-6}	1.71×10^{-6}
MF	GO:0048018	receptor ligand activity	93/974	482/17,697	4.83×10^{-27}	3.72×10^{-24}	3.13×10^{-24}
MF	GO:0005125	cytokine activity	54/974	220/17,697	4.18×10^{-21}	1.61×10^{-18}	1.36×10^{-18}
MF	GO:0005201	extracellular matrix structural constituent	44/974	163/17,697	3.78×10^{-19}	9.72×10^{-17}	8.17×10^{-17}
MF	GO:0005126	cytokine receptor binding	55/974	286/17,697	2.45×10^{-16}	4.73×10^{-14}	3.98×10^{-14}
MF	GO:0008009	chemokine activity	21/974	49/17,697	2.60×10^{-14}	4.00×10^{-12}	3.37×10^{-12}

GO, Gene Ontology; BP, biological process; CC, cellular component; MF, molecular function; MHC, major histocompatibility complex.

Table 3. KEGG enrichment analysis.

ONTOLOGY	ID	Description	GeneRatio	BgRatio	*p* value	*p*.adjust	q.value
KEGG	hsa04060	Cytokine-cytokine receptor interaction	70/495	295/8076	4.35×10^{-24}	1.21×10^{-21}	9.80×10^{-22}
KEGG	hsa04061	Viral protein interaction with cytokine and cytokine receptor	36/495	100/8076	3.30×10^{-19}	4.60×10^{-17}	3.71×10^{-17}
KEGG	hsa04640	Hematopoietic cell lineage	33/495	99/8076	1.54×10^{-16}	1.43×10^{-14}	1.15×10^{-14}
KEGG	hsa04672	Intestinal immune network for IgA production	20/495	49/8076	2.06×10^{-12}	1.43×10^{-10}	1.16×10^{-10}
KEGG	hsa04940	Type I diabetes mellitus	18/495	43/8076	1.60×10^{-11}	7.48×10^{-10}	6.04×10^{-10}

KEGG, Kyoto Encyclopedia of Genes and Genomes.

Sensitivity of CYP26A1 and Hub Genes to Chemotherapeutic Drugs and Small-Molecule Compounds

We downloaded mRNA expression profiles and drug activity data for *CYP26A1* from the CellMiner database. The correlations between *CYP26A1* expression levels and compound sensitivity were evaluated by Pearson correlation coefficients, with $p < 0.05$ as the threshold for significance. *VCAN*, *COL1A1*, *COL1A2* and *CYP26A1* expression levels were correlated with the sensitivity of most, but not all, of the chemotherapeutic and small-molecule compounds tested (Fig. 8A–P). Moreover, the relationships between *CYP26A1* expression, hub gene expression, and sensitivity to small-molecule drugs were visualized using CellMiner (Fig. 9A–P).

Discussion

Rapid advances in molecular biology have enabled the discovery of assorted tumor-related diagnostic and therapeutic biomarkers. Given that various cancers involve the abnormal expression of *CYP26A1*, including breast cancer [19], colorectal cancer [35], skin cancer [36], bladder cancer [37], cervical cancer, and pancreatic cancer [20], we hypothesized that *CYP26A1* is a candidate oncogene. However, the association between *CYP26A1* and THCA has not yet been established. In our study, TCGA was used to obtain high-throughput RNA-seq sequencing data for evaluating the prognostic value of *CYP26A1* in THCA. We found that increased *CYP26A1* expression in THCA was associated with poor clinical pathological features, such as PFI, tumor stage, cervical lymph node metastasis, and extraglandular invasion. Thus, our results highlighted a role of *CYP26A1* in THCA and suggest its potential as a diagnostic or prognostic biomarker.

CYP26A1 belongs to the cytochrome P450 superfamily, containing eight exons [38]. In the adult, CYP26A1 is highly expressed in the liver and at lower levels in the brain and testis, whereas CYP26B1 is predominantly expressed in brain tissue, with lower expression in other tissues [39]. *CYP26A1* can inactivate RA, thereby limiting the bioavailability of RA and disrupting the maintenance of RA homeostasis [40]. RA, an active metabolite of vitamin A, plays a critical role in the immune system, cell proliferation and differentiation, and embryonic development by activating nuclear receptors to initiate and regulate

Table 4. GSEA analysis.

Description	Set Size	Enrichment Score	NES	*p* value	*p*.adjust
HALLMARK_ALLOGRAFT_REJECTION	200	0.77719775	2.19170502	0.00102775	0.00399042
HALLMARK_INTERFERON_GAMMA_RESPONSE	200	0.75855372	2.13912869	0.00102775	0.00399042
HALLMARK_INTERFERON_ALPHA_RESPONSE	97	0.75568375	2.03664417	0.00109649	0.00399042
HALLMARK_EPITHELIAL_MESENCHYMAL_TRANSITION	200	0.72869365	2.05492298	0.00102775	0.00399042
HALLMARK_INFLAMMATORY_RESPONSE	199	0.71673612	2.01781772	0.00102987	0.00399042
HALLMARK_ANGIOGENESIS	36	0.70877688	1.7121326	0.00124224	0.00414079
HALLMARK_IL6_JAK_STAT3_SIGNALING	87	0.686675	1.82248689	0.00111732	0.00399042
HALLMARK_TNFA_SIGNALING_VIA_NFKB	200	0.64455048	1.81763847	0.00102775	0.00399042
HALLMARK_KRAS_SIGNALING_UP	200	0.63883895	1.80153188	0.00102775	0.00399042
HALLMARK_COMPLEMENT	200	0.60972744	1.71943715	0.00102775	0.00399042
HALLMARK_COAGULATION	138	0.58850817	1.63021212	0.00105374	0.00399042
HALLMARK_IL2_STAT5_SIGNALING	198	0.58824392	1.65727604	0.00102775	0.00399042
HALLMARK_MYOGENESIS	199	0.5728483	1.61273225	0.00102987	0.00399042
HALLMARK_APOPTOSIS	161	0.56993311	1.59558475	0.00103627	0.00399042
HALLMARK_APICAL_JUNCTION	199	0.54745728	1.54124926	0.00102987	0.00399042
HALLMARK_KRAS_SIGNALING_DN	199	0.51198979	1.44139809	0.0030896	0.00965499
HALLMARK_P53_PATHWAY	199	0.48949213	1.37806071	0.00720906	0.02120313
HALLMARK_UNFOLDED_PROTEIN_RESPONSE	112	–0.3678885	–1.36773	0.01408451	0.03912363

GSEA, gene set enrichment analysis; NES, normalized enrichment score.

Table 5. Logistics regression to identify clinical features associated with *CYP26A1* expression.

Characteristic	Total (N)	Odds Ratio (OR)	*p* value
T stage (T3&T4 vs. T1&T2)	508	1.670 (1.166–2.397)	0.005
N stage (N1 vs. N0)	460	1.442 (1.000–2.085)	0.051
M stage (M1 vs. M0)	295	0.648 (0.158–2.497)	0.524
Gender (Male vs. Female)	510	0.942 (0.638–1.392)	0.765
Age (>45 years vs. ≤45 years)	510	1.393 (0.983–1.976)	0.063
Extrathyroidal extension (Yes vs. No)	492	2.220 (1.504–3.300)	<0.001

gene expression [41], and functions in the formation and maintenance of tissues. Interruption of the RA signaling pathway is implicated in the etiology of many tumors [42], including leukemia, skin cancer, head and neck neoplasms, lung carcinoma, breast carcinoma, ovarian carcinoma, prostatic carcinoma, and kidney cancer. The *CYP26A1* gene promoter contains an RA response element (RARE) and serves as a suitable instrument to determine RAR-mediated retinoid activity [43]. Upon activation, this promoter recruits transcriptional machinery to the Sp1/Sp3 binding site, thereby inducing *CYP26A1* gene expression [44]. Although the functional consequences of high *CYP26A1* expression and activity in carcinoma cells remain unclear, clinical observations suggested that *CYP26A1*-mediated catabolism may be involved in the tumor-inhibiting effect of endogenous RA and its therapeutic efficacy [45]. Our outcomes indicated that *CYP26A1* was highly expressed in most tumors. Given the regulatory mechanism linking *CYP26A1* to RA, *CYP26A1* was a potential diagnostic marker for various cancers *CYP26A1* and may also serve as a biomarker in THCA.

To identify the mechanism and effects of *CYP26A1* in THCA, we performed a differential expression analysis and identified 685 upregulated genes and 109 downregulated genes in the high *CYP26A1* expression group. Furthermore, GO and KEGG functional enrichment analyses of the DEGs were performed. The most highly enriched KEGG pathways were type I diabetes mellitus, intestinal immune network for IgA production, hematopoietic cell lineage, viral protein interaction with cytokine and cytokine receptor, and cytokine-cytokine receptor interaction. Enriched GO terms included biological processes (e.g., cell chemotaxis, lymphocyte differentiation, extracellular matrix organization, and extracellular structure organization), cellular components (e.g., collagen trimer, endoplasmic reticulum lumen, external side of plasma membrane, and collagen-containing extracellular matrix), and molecular functions (e.g., extracellular matrix structural constituent, cytokine activity, cytokine receptor binding, and receptor ligand activity).

Cytokines are major regulators of the innate and adaptive immune systems, allowing short-range communication within the immune system through autocrine and paracrine signaling [46]. Extracellular matrix components can promote tumor progression and metastasis by regulating the MAPK/ERK signaling pathway [47]. Dysregulation of the cell cycle, particularly the mitotic phase, plays impor-

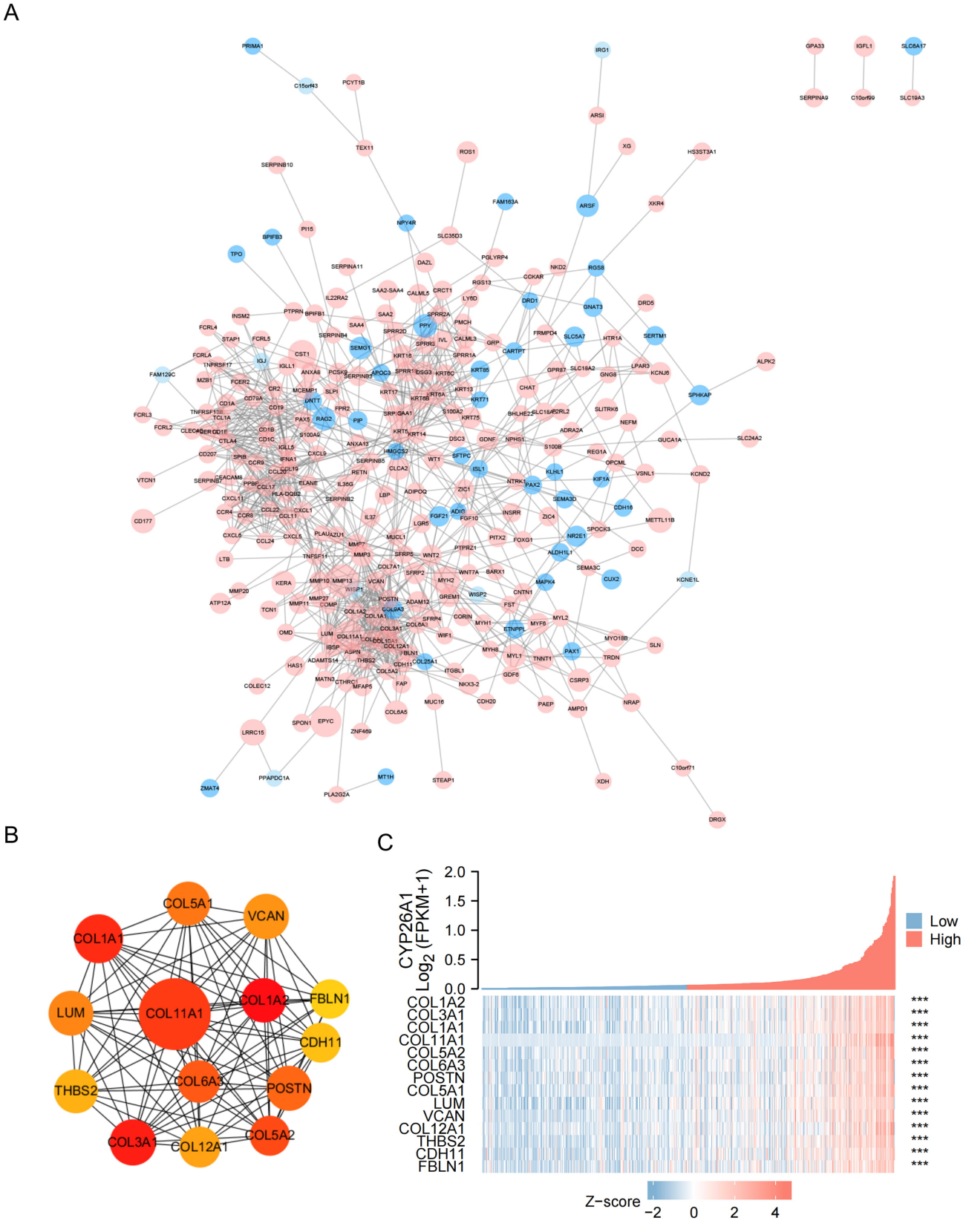

Fig. 4. Protein-Protein interaction (PPI) network. (A) The PPI was constructed by the STRING database for differential genes. PPI results were extracted from the STRING database and visualized by Cytoscape; the node shape and size were proportional to the multiple of difference (blue = down-regulated genes in the group with high *CYP26A1* expression). (B) Analyses (CytoHubba plug-in) of the top 14 central genes obtained by maximum correlation criteria (MCC) (darker color = higher MCC score). (C) Heat map of co-expression of *CYP26A1* genes and Hub genes. ***$p < 0.001$.

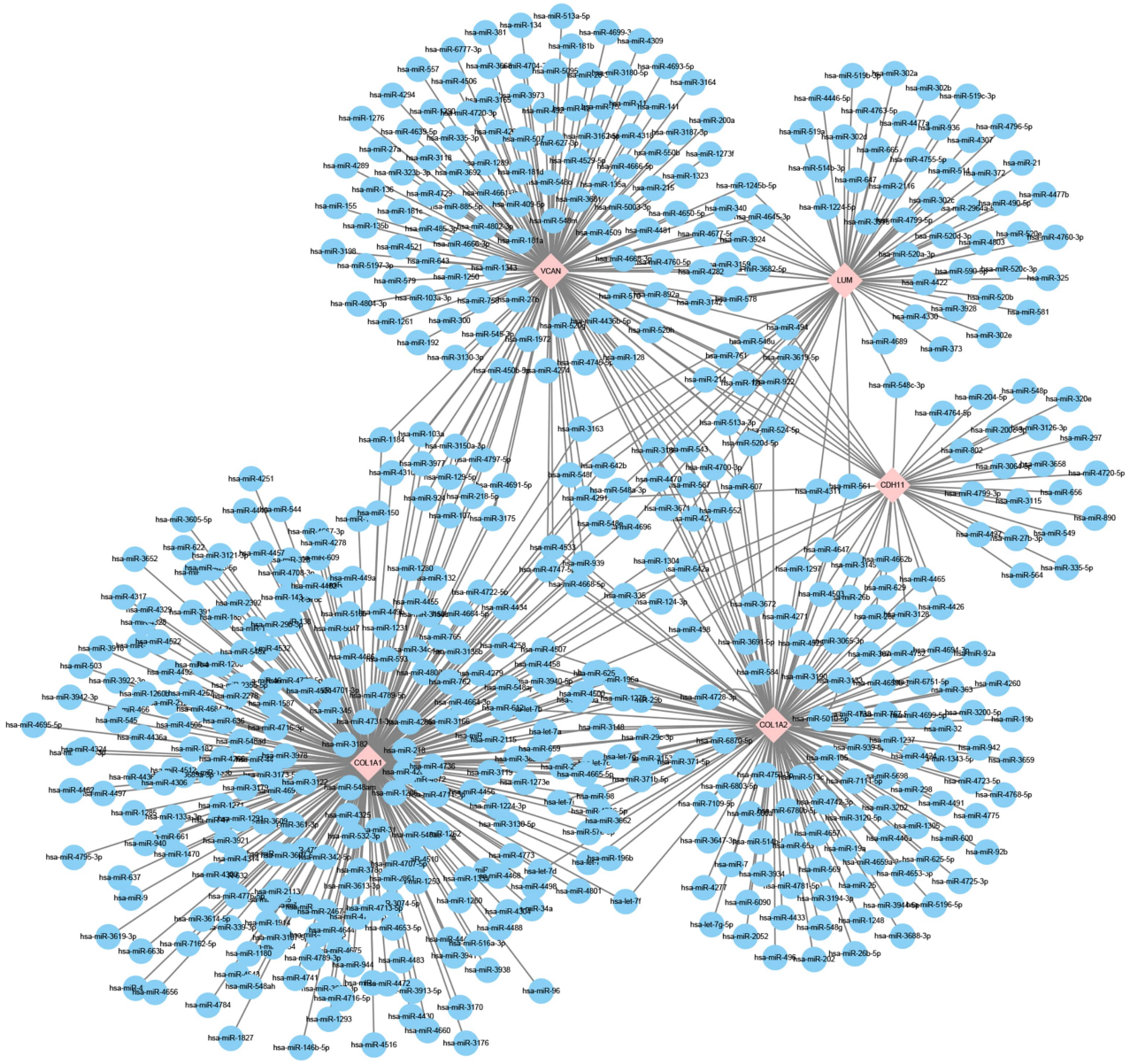

Fig. 5. Differential gene-miRNA regulatory network. The pink diamond node = Hub gene, and the blue round node = corresponding miRNA.

tant roles in tumorigenesis and cancer progression [48]. In addition, oxidoreductase activity is vital in antioxidant defense and could contribute to tumor suppression [49]. Herein, GSEA results showed that *CYP26*A1 was related to genes in the KRAS, P53 and apoptotic signaling pathways, which were closely related to THCA. KRAS can transmit stimulatory signals from upstream molecules into cells, thereby regulating proliferation, differentiation, survival, apoptosis, and other biological activities. Mutations in the *KRAS* gene can cause overexpression and continuous activation of the KRAS protein, which in turn activates downstream signaling pathways. This activation promotes uncontrollable proliferation, malignant transformation, and ultimately contributes to tissue carcinogenesis. Accordingly, *CYP26A1* affected multiple signaling pathways, *CYP26A1* and induced oncogenes, including c-Myc and epidermal growth factor receptor, thereby regulating cell cycle and DNA repair; these results support the notion that *CYP26A1* promotes cell survival via anti-apoptotic signaling [50]. However, when RA catabolism is enhanced and the RA level is deficient, apoptosis may be limited, leading to the accumulation of DNA damage under vitamin A deficiency [51]. We constructed a PPI network of *CYP26A1*-related genes and an mRNA–miRNA network of DEGs. The first 20 hub genes were obtained, including genes involved in various signaling pathways and biological processes, and their expression levels were all significantly correlated with *CYP26A1* levels. Therefore, we hypothesized that *CYP26A1* may be a key hub gene in THCA.

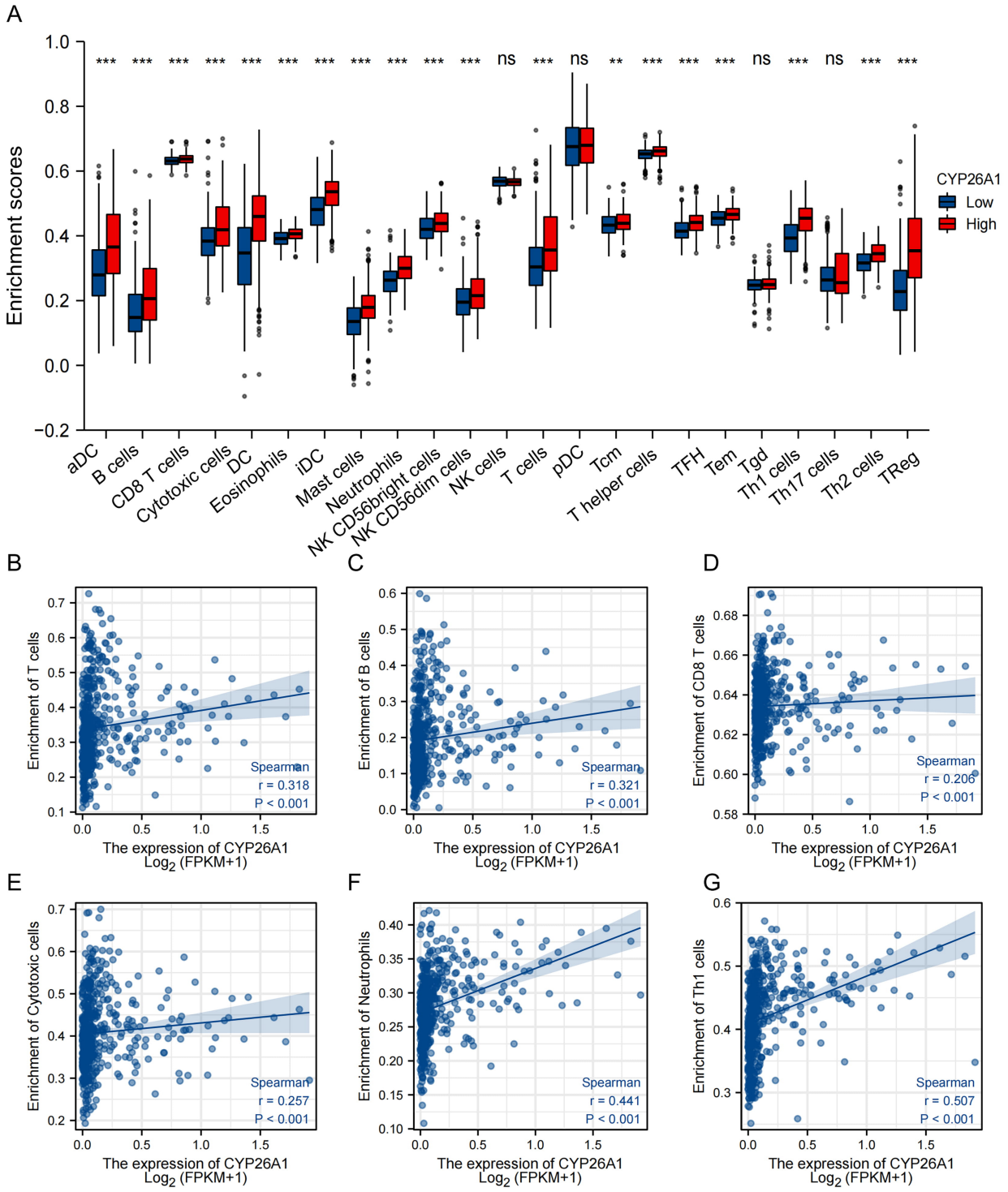

Fig. 6. Immune cell infiltration analysis. (A) Differences in the enrichment and abundance of immune cells (red = the group with highly expressed *CYP26A1*, blue = the group with lowly expressed *CYP26A1*, the horizontal axis = various immune cells, and the vertical axis = the abundance of immune cell infiltration). (B–G) Correlation analysis between *CYP26A1* and the vertical axis as the abundance of immune cell infiltration. $^{**}p < 0.01$, $^{***}p < 0.001$, ns, not significant.

The tumor microenvironment is instrumental in mediating tumor progression, with immune cells constituting an integral component [52]. Epidemiological and clinical information suggested that THCA involves spontaneous antitumor immune responses and tumor immune escape mechanisms [53]. To evaluate immune infiltration differences with respect to *CYP26A1* expression, we employed ssGSEA and found a correlation between *CYP26A*1 expression and the abundance of immune cells (T cells, B cells, CD8 T cells, cytotoxic cells, neutrophils, and Th1 cells).

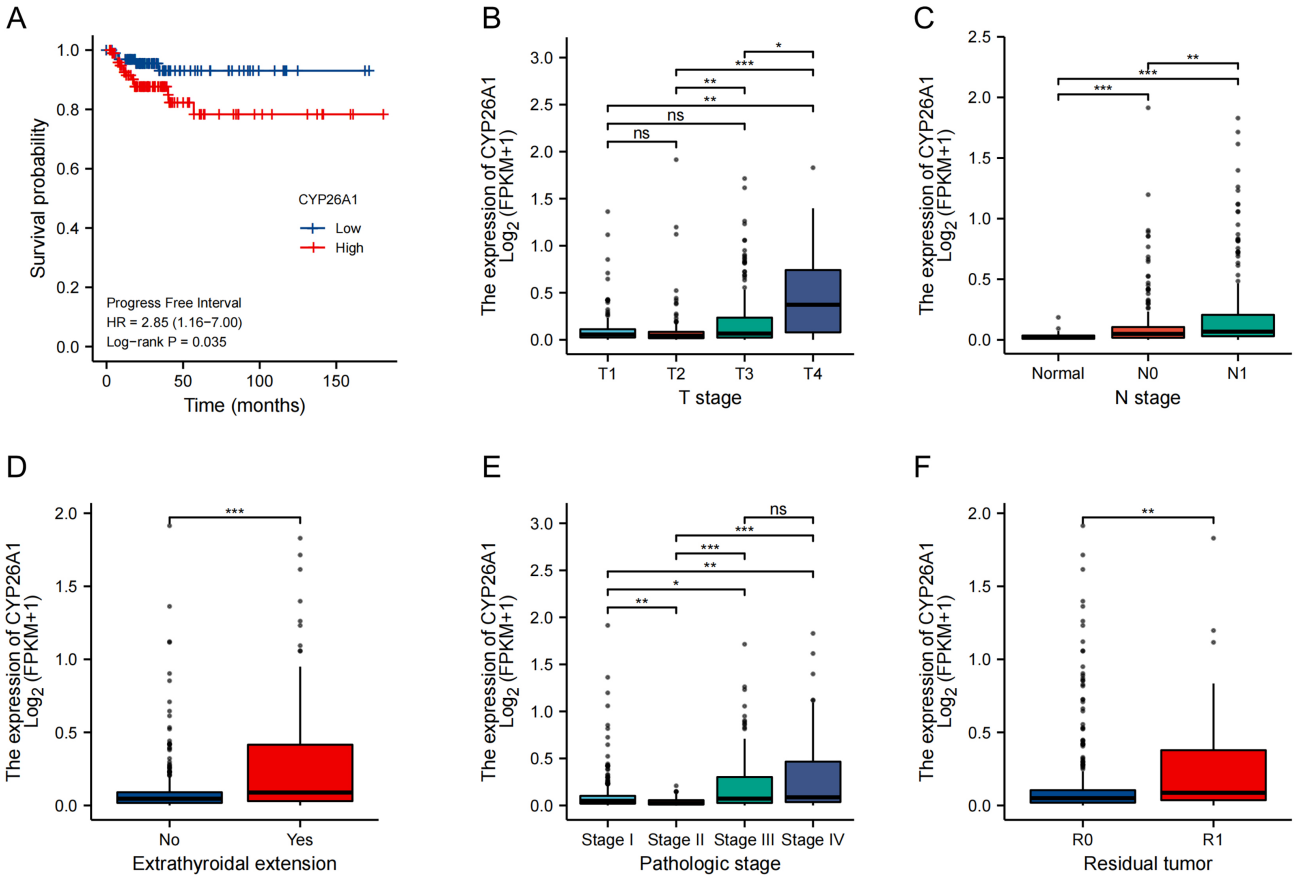

Fig. 7. High *CYP26A1* expression was associated with the pathological features of invasive tumors, such as cervical lymph node metastasis and extra-glandular invasion of THCA. (A) Survival analysis of *CYP26A1* gene expression (blue line = low expression; red line = high expression; horizontal axis = time; vertical axis = survival probability). (B) Differences in *CYP26A1* gene expression in different T stages of THCA. (C) Differences in *CYP26A1* gene expression in different N stages (cervical lymph node metastasis) in THCA. (D) Differences in *CYP26A1* gene expression in THCA tissues with extrathyroidal extension. (E) Differences in *CYP26A1* gene expression among pathological grades of THCA. (F) Differences in *CYP26A1* gene expression across resection margin statuses in THCA. $^{*}p < 0.05$, $^{**}p < 0.01$, $^{***}p < 0.001$, ns, not significant.

These immune cells play crucial roles in cancer control, suggesting that *CYP26A1* participates in the occurrence and development of THCA via alterations in immune cell infiltration. B cells are part of a core immune cell network and have been linked to longer survival in THCA. Targeting CD4(+) T helper cells enhances the induction of a dendritic cell antineoplastic reaction and improves clinical outcomes [54]. Dendritic cells are typical antigen-presenting cells that initiate anti-tumor immunity by cross-priming CD8+ cells [55]. In the ensuing immune response, neutrophils and macrophages cooperate to protect against the tumor growth [56]. In different cancers, neutrophils are associated with a better prognosis [57]. *CYP26A1* is associated with increased cell survival, and its upregulation affects gene expression signatures in tumor cells, probably generating multiple concrete and powerful pro-survival signals, and conferring a selective growth advantage. *CYP26A1* can suppress tumor immunity, aid cancer cell escape from elimination, and promote tumorigenesis, and may influence the immune microenvironment by regulating the activity of NK cells [38]. CYP26A1 is also related to the infiltration of inflammatory cells, including neutrophils and T lymphocytes, in skin diseases [40]. These results demonstrate the relationship between *CYP26A1* expression and the level of immune cell infiltration, providing a reference for THCA immunotherapy.

The clinical value of *CYP26A1* in THCA has not been established. Our results indicated that *CYP26A1* had a predictive value for distinguishing between tumor tissues and normal tissues (AUC of 0.734), showing that *CYP26A1* was an effective biomarker. Furthermore, the PFI, T stage (i.e., T3 and T4 stages), cervical lymph node metastasis, and extra-glandular invasion were associated with high *CYP26A1* expression. We also conducted a sensitivity analysis and demonstrated that *CYP26A1* and hub gene expression levels were pertinent to chemotherapeutic drugs and small-molecule compounds. The correlations between genes and small drug molecules revealed that *CYP26A1*

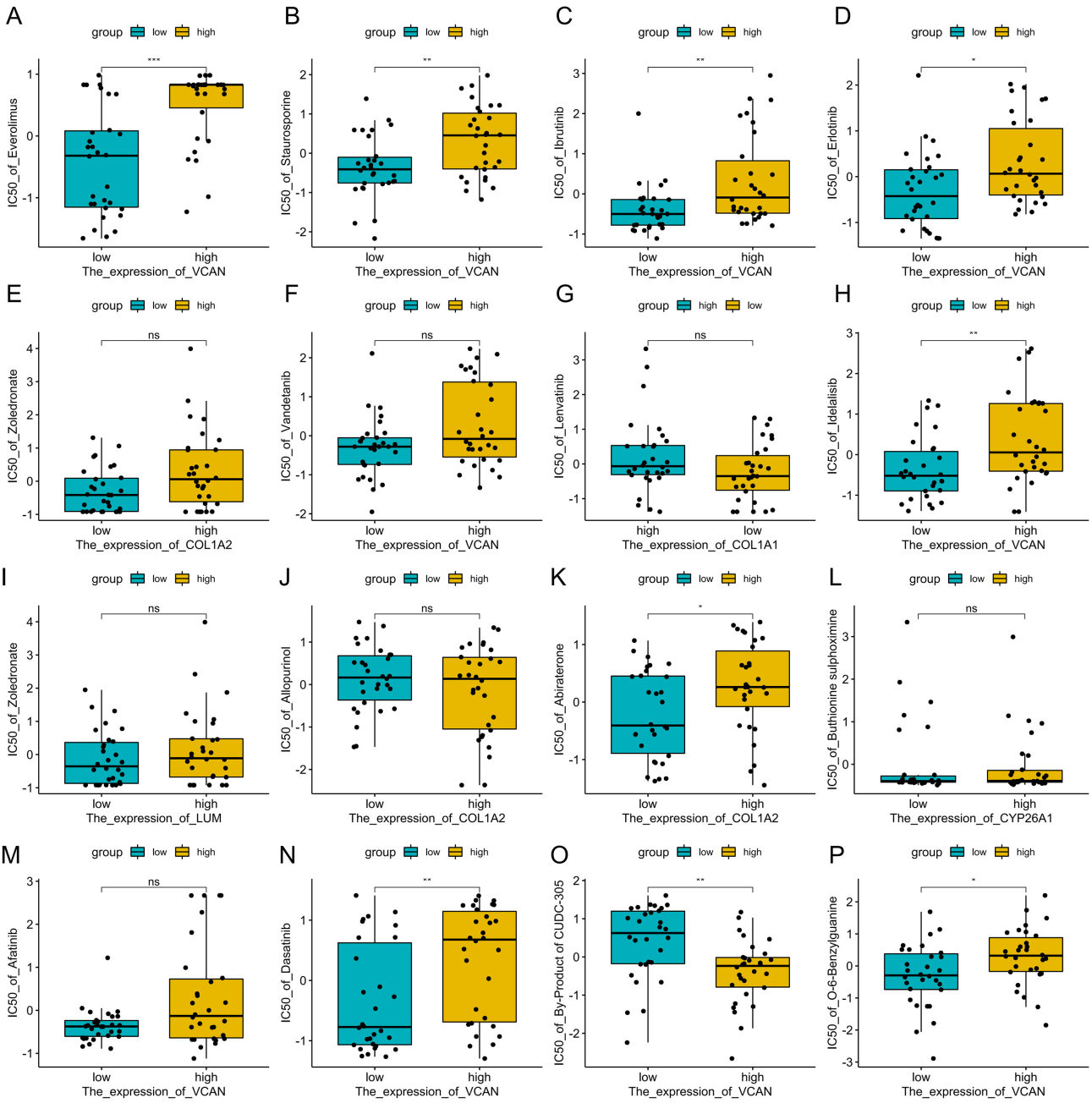

Fig. 8. *CYP26A1* expression, Hub gene expression, and sensitivity analysis to chemotherapeutic drugs and small-molecule compounds. (A–P) Drug sensitivity of *CYP26A1* and its related genes (horizontal axis = the grouping of gene expression; vertical axis = the IC50 value of the drug). *$p < 0.05$, **$p < 0.01$, ***$p < 0.001$, ns, not significant.

may be a potential therapeutic target for suppressing the malignant potential of *CYP26A1*-overexpressing human tumors [19].

In recent years, a study has also explored the roles of other biomarkers (BRAF V600E and TERT promoter mutations) in the diagnosis and prognosis of THCA [58]. Compared with these established molecular markers, this study systematically revealed, for the first time, the independent prognostic value of *CYP26A1* in THCA and its association with the immune microenvironment. The advantage of *CYP26A1* lies in its functional plasticity as a key enzyme in RA metabolism, which may simultaneously reflect the intrinsic metabolic abnormalities and immune regulation imbalances in tumor cells, providing a novel perspective for understanding the progression of THCA. However, compared with established biomarkers, the clinical validation of *CYP26A1* in THCA remains in its early stages. The standardization of its detection, tissue specificity, and the combined application value with existing markers still need to be clarified through subsequent large-sample studies.

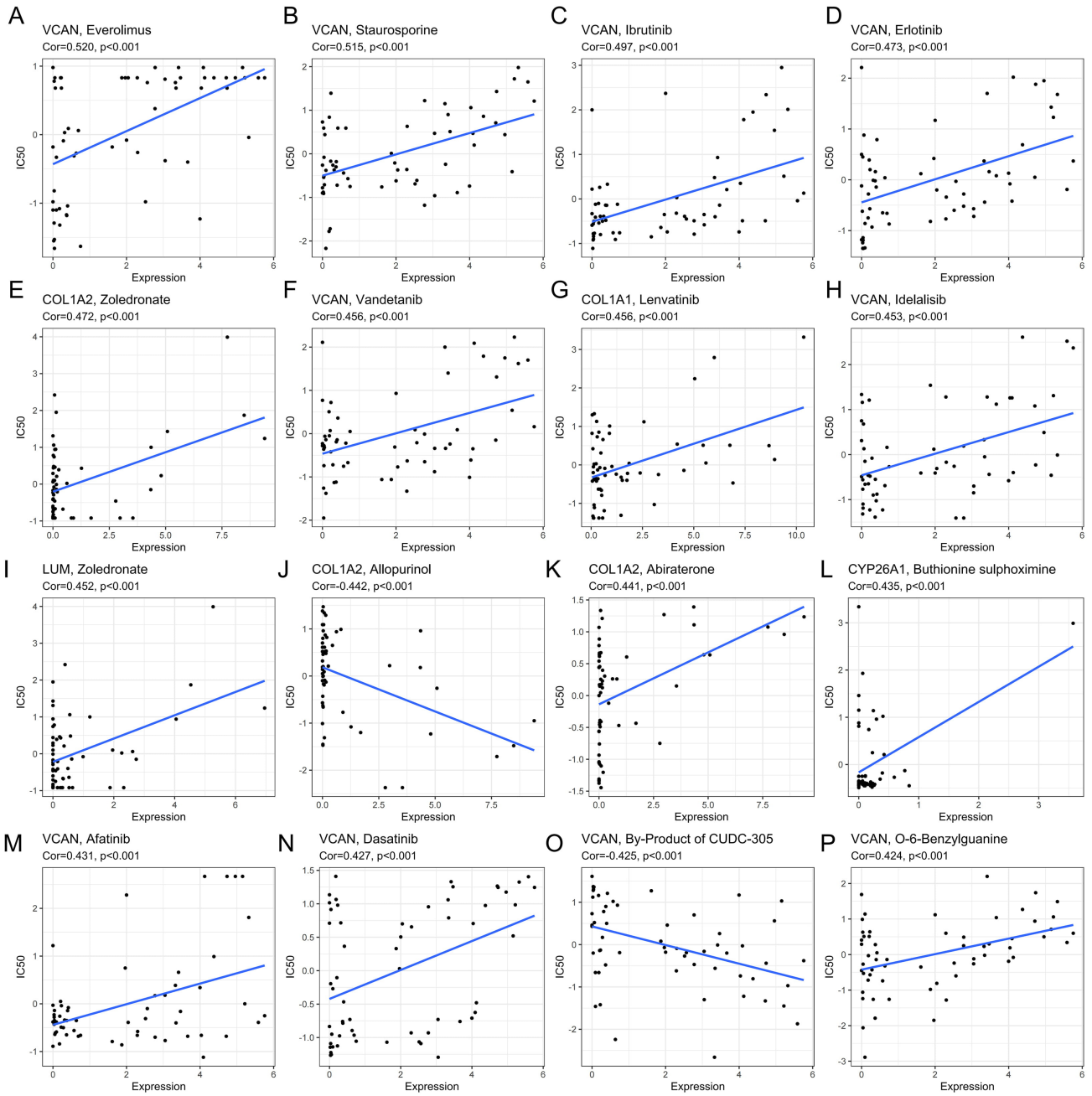

Fig. 9. Correlation analysis of *CYP26A1* and Hub gene expression and sensitivity to chemotherapeutic drugs and small-molecule compounds. (A–P) Drug sensitivity of *CYP26A1* and its related genes (horizontal axis = gene expression level; vertical axis = drug IC50 value).

Although this study revealed a significant relationship between *CYP26A1* and THCA, some limitations should be noted. First, *in vitro* cell experiments and clinical sample validation were not performed to verify the role of CYP26A1 in THCA cell behaviors and prognosis. Therefore, its biological function and clinical value remain to be further confirmed. Second, key clinical treatment-related factors, including radioactive iodine therapy status, surgical approaches, and other adjuvant therapies, underwent no correlation and prognostic analyses. Third, no independent cohorts, such as GEO datasets, were included for external validation. Thus, the differential expression and prognostic value of CYP26A1 still require external verification. Other key signaling pathways associated with cancers also require further exploration. Finally, batch effects could not be fully eliminated [59]; in the statistical analyses, we removed the batch effects using the limma package's in-built function, which weakened these effects to a certain extent.

Conclusion

In conclusion, high *CYP26A1* expression is associated with THCA occurrence and may have prognostic value, suggesting its potential as a therapeutic target.

Availability of Data and Materials

Publicly available datasets were analyzed in this study. This data can be found at https://portal.gdc.cancer.gov/ and http://genome.ucsc.edu.

Author Contributions

TC and YZ designed the research study; WL and DZ performed the research; HG and YZ collected and analyzed the data. TC has been involved in drafting the manuscript and all authors have been involved in revising it critically for important intellectual content. All authors gave final approval of the version to be published. All authors have participated sufficiently in the work to take public responsibility for appropriate portions of the content and agreed to be accountable for all aspects of the work in ensuring that questions related to its accuracy or integrity.

Ethics Approval and Consent to Participate

Not applicable.

Acknowledgment

Not applicable.

Funding

This research received no external funding.

Conflict of Interest

The authors declare no conflict of interest.

References

[1] Pan Y, Wu L, He S, Wu J, Wang T, Zang H. Identification of hub genes in thyroid carcinoma to predict prognosis by integrated bioinformatics analysis. Bioengineered. 2021; 12: 2928–2940. https://doi.org/10.1080/21655979.2021.1940615.

[2] Ramírez-Moya J, Miliotis C, Baker AR, Gregory RI, Slack FJ, Santisteban P. An ADAR1-dependent RNA editing event in the cyclin-dependent kinase CDK13 promotes thyroid cancer hallmarks. Molecular Cancer. 2021; 20: 115. https://doi.org/10.1186/s12943-021-01401-y.

[3] Kitahara CM, Sosa JA. The changing incidence of thyroid cancer. Nature Reviews. Endocrinology. 2016; 12: 646–653. https://doi.org/10.1038/nrendo.2016.110.

[4] Zhang J, Gill A, Atmore B, Johns A, Delbridge L, Lai R, *et al*. Upregulation of the signal transducers and activators of transcription 3 (STAT3) pathway in lymphatic metastases of papillary thyroid cancer. International Journal of Clinical and Experimental Pathology. 2011; 4: 356–362.

[5] Zhou T, Zhao DW, Ma N, Zhu XY, Chen XH, Luo X, *et al*. The essential role of forkhead box P4 (FOXP4) in thyroid cancer: a study related to The Cancer Genome Atlas and experimental data. Endocrine Connections. 2023; 12: e220390. https://doi.org/10.1530/EC-22-0390.

[6] Su X, Jiang X, Xu X, Wang W, Teng X, Shao A, *et al*. Diagnostic value of BRAF (V600E)-mutation analysis in fine-needle aspiration of thyroid nodules: a meta-analysis. OncoTargets and Therapy. 2016; 9: 2495–2509. https://doi.org/10.2147/OTT.S101800.

[7] Qi F, Tang J, Cai Z, Wang G, Wang Z. Long non-coding RNA CATIP antisense RNA 1 (lncRNA CATIP-AS1) downregulation contributes to the progression and metastasis of thyroid cancer via epithelial-mesenchymal transition (EMT) pathway. Bioengineered. 2022; 13: 7592–7606. https://doi.org/10.1080/21655979.2022.2047400.

[8] Zhang B, Liu T, Gu Y, Ren L, Wang J, Feng C, *et al*. Long Non-Coding RNA LPP-AS2 Plays an Anti-Tumor Role in Thyroid Carcinoma by Regulating the miR-132-3p/OLFM1 Axis. Critical Reviews in Eukaryotic Gene Expression. 2023; 33: 73–86. https://doi.org/10.1615/CritRevEukaryotGeneExpr.v33.i5.70.

[9] Zhang B, Li Q, Song Z, Ren L, Gu Y, Feng C, *et al*. hsa_circ_0000285 facilitates thyroid cancer progression by regulating miR-127-5p/CDH2. Journal of Clinical Laboratory Analysis. 2022; 36: e24421. https://doi.org/10.1002/jcla.24421.

[10] Han C, Mo K, Jiang L, Wang K, Teng L. miR-183-5p promotes proliferation, invasion, and glycolysis of thyroid carcinoma cells by targeting FOXO1. Molecular and Cellular Biochemistry. 2022; 477: 1195–1206. https://doi.org/10.1007/s11010-022-04357-9.

[11] Luo X, Chen X, Chen S, Gao Q, Yang H, Zhao D. High expression of *SEZ6L2* as an independent prognostic Indicator in thyroid carcinoma. Gland Surgery. 2022; 11: 412–425. https://doi.org/10.21037/gs-22-37.

[12] Sun R, Yang L, Hu Y, Wang Y, Zhang Q, Zhang Y, *et al*. ANGPTL1 is a potential biomarker for differentiated thyroid cancer diagnosis and recurrence. Oncology Letters. 2020; 20: 240. https://doi.org/10.3892/ol.2020.12103.

[13] Li ZY, Liu WZ, Guang H, Chen WC, Yang YH. Silencing of long noncoding RNA H19 inhibited invasion and migration of papillary thyroid cancer cells via microRNA-138-dependent regulating of LRRK2. Journal of Biological Regulators and Homeostatic Agents. 2021; 35: 253–258. https://doi.org/10.23812/20-422-L.

[14] Liu X, Yang M, Guo Y, Lu X. Annexin A10 is a novel prognostic biomarker of papillary thyroid cancer. Irish Journal of Medical Science. 2021; 190: 59–65. https://doi.org/10.1007/s11845-020-02263-x.

[15] White JA, Guo YD, Baetz K, Beckett-Jones B, Bonasoro J, Hsu KE, *et al*. Identification of the retinoic acid-inducible all-trans-retinoic acid 4-hydroxylase. The Journal of Biological Chemistry. 1996; 271: 29922–29927. https://doi.org/10.1074/jbc.271.47.29922.

[16] Takahashi N, Saito D, Hasegawa S, Yamasaki M, Imai M. Vitamin A in health care: Suppression of growth and induction of differentiation in cancer cells by vitamin A and its derivatives and their mechanisms of action. Pharmacology & Therapeutics. 2022; 230: 107942. https://doi.org/10.1016/j.pharmthera.2021.107942.

[17] Bauzone M, Souidi M, Dessein AF, Wisztorski M, Vincent A, Gimeno JP, *et al*. Cross-talk between YAP and RAR-RXR Drives Expression of Stemness Genes to Promote 5-FU Resistance and Self-Renewal in Colorectal Cancer Cells. Molecular Cancer Research. 2021; 19: 612–622. https://doi.org/10.1158/1541-7786.MCR-20-0462.

[18] Facey COB, Hunsu VO, Zhang C, Osmond B, Opdenaker LM, Boman BM. *CYP26A1* Links WNT and Retinoic Acid Signaling: A Target to Differentiate ALDH+ Stem Cells in *APC*-Mutant CRC. Cancers. 2024; 16: 264. https://doi.org/10.3390/cancers16020264.

[19] Osanai M, Sawada N, Lee GH. Oncogenic and cell survival properties of the retinoic acid metabolizing enzyme, CYP26A1. Oncogene. 2010; 29: 1135–1144. https://doi.org/10.1038/onc.2009.414.

[20] Yu Y, Wang Y, Zou Y, Yu Y. CYP26A1 Is a Novel Cancer Biomarker of Pancreatic Carcinoma: Evidence from Integration Analysis and *In Vitro* Experiments. Disease Markers. 2022; 2022: 5286820. https://doi.org/10.1155/2022/5286820.

[21] Feng JL, Zheng WJ, Xu L, Zhou QY, Chen J. Identification of potential LncRNAs as papillary thyroid carcinoma biomarkers based on integrated bioinformatics analysis using TCGA and RNA sequencing data. Scientific Reports. 2023; 13: 4350. https://doi.org/10.1038/s41598-023-30086-0.

[22] Xu S, Deng C, Man Z, Yang S, Xu M. To develop prognostic markers related to drug resistance in pancreatic cancer patients based on multiple machine learning methods. Annals of Medicine and Surgery (2012). 2025; 87: 8170–8189. https://doi.org/10.1097/MS9.0000000000004051.

[23] Yang Y, Jing W, Zhang L, Zhang Y, Shang Y, Kuang Y. WDR62 affects the progression of ovarian cancer by regulating the cell cycle. Hereditas. 2025; 162: 78. https://doi.org/10.1186/s41065-025-00444-1.

[24] Bertilsson F, Hikmet F, Hansen JN, Uhlén M, Méar L, Lindskog C. A High-Resolution Subcellular Map of Proteins in Cells with Motile Cilia. Journal of Proteome Research. 2026; 25: 231–243. https://doi.org/10.1021/acs.jproteome.5c00686.

[25] Cui X, Sawashita J, Dai J, Liu C, Igarashi Y, Mori M, *et al*. Exercise suppresses mouse systemic AApoAII amyloidosis through enhancement of the p38 MAPK signaling pathway. Disease Models & Mechanisms. 2022; 15: dmm049327. https://doi.org/10.1242/dmm.049327.

[26] Zhang X, Wang L, Yang T, Kong L, Wei L, Du J. Bioinformatic analysis of the role of immune checkpoint genes and immune infiltration in the pathogenesis and development of premature ovarian insufficiency. Journal of Assisted Reproduction and Genetics. 2024; 41: 1619–1635. https://doi.org/10.1007/s10815-024-03120-x.

[27] Wang Z, Yuan C, Xu T, Xie W, Wu J, Wang H. Bioinformatics analysis and experimental validation of ferroptosis genes in heart failure and atrial fibrillation. Frontiers in Genetics. 2025; 16: 1541342. https://doi.org/10.3389/fgene.2025.1541342.

[28] Zhu S, Zhang G, You Q, Li F, Ding B, Liu F, *et al*. Stemness-related gene signature for predicting therapeutic response in patients with esophageal cancer. Translational Cancer Research. 2022; 11: 2359–2373. https://doi.org/10.21037/tcr-22-1723.

[29] Chen Z, Wang X, Li L, Han M, Wang M, Li Z, *et al*. Construction of an autophagy interaction network based on competitive endogenous RNA reveals the key pathways and central genes of SARS-CoV-2 infection in vivo. Microbial Pathogenesis. 2021; 158: 105051. https://doi.org/10.1016/j.micpath.2021.105051.

[30] Cai Y, Zuo X, Zuo Y, Wu S, Pang W, Ma K, *et al*. Transcriptomic analysis reveals shared gene signatures and molecular mechanisms between obesity and periodontitis. Frontiers in Immunology. 2023; 14: 1101854. https://doi.org/10.3389/fimmu.2023.1101854.

[31] Yue T, Cai Y, Zhu J, Liu Y, Chen S, Wang P, *et al*. Autophagy-related IFNG is a prognostic and immunochemotherapeutic biomarker of COAD patients. Frontiers in Immunology. 2023; 14: 1064704. https://doi.org/10.3389/fimmu.2023.1064704.

[32] Zhou Q, Shi R. Shared Genetic Features of Psoriasis and Myocardial Infarction: Insights From a Weighted Gene Coexpression Network Analysis. Journal of the American Heart Association. 2024; 13: e033893. https://doi.org/10.1161/JAHA.123.033893.

[33] Li J, Li B, Zhao R, Li G. Systematic analysis of the aberrances and functional implications of cuproptosis in cancer. iScience. 2023; 26: 106319. https://doi.org/10.1016/j.isci.2023.106319.

[34] Cheng M, Liu Y, Guo Y, Li M, Xian S, Qin H, *et al*. Pan-cancer analysis reveals signal transducer and activator of transcription (STAT) gene family as biomarkers for prognostic prediction and therapeutic guidance. Frontiers in Genetics. 2023; 14: 1120500. https://doi.org/10.3389/fgene.2023.1120500.

[35] Zhu Y, Zhou T, Zheng Y, Yao Y, Lin M, Zeng C, *et al*. Folate metabolism-associated CYP26A1 is a clinico-immune target in colorectal cancer. Genes and Immunity. 2025; 26: 376–393. https://doi.org/10.1038/s41435-025-00342-6.

[36] Wang Z, Boudjelal M, Kang S, Voorhees JJ, Fisher GJ. Ultraviolet irradiation of human skin causes functional vitamin A deficiency, preventable by all-trans retinoic acid pre-treatment. Nature Medicine. 1999; 5: 418–422. https://doi.org/10.1038/7417.

[37] Ozgun G, Senturk S, Erkek-Ozhan S. Retinoic acid signaling and bladder cancer: Epigenetic deregulation, therapy and beyond. International Journal of Cancer. 2021; 148: 2364–2374. https://doi.org/10.1002/ijc.33374.

[38] Li DD, Ji WH, Wei DP, Gu AQ, Song ZH, Fang WN, *et al*. Cytochrome P450 26A1 regulates the clusters and killing activity of NK cells during the peri-implantation period. Journal of Cellular and Molecular Medicine. 2022; 26: 2438–2450. https://doi.org/10.1111/jcmm.17269.

[39] Cao DL, Ma LJ, Jiang BC, Gu Q, Gao YJ. Cytochrome P450 26A1 Contributes to the Maintenance of Neuropathic Pain. Neuroscience Bulletin. 2024; 40: 293–309. https://doi.org/10.1007/s12264-023-01101-1.

[40] Snyder JM, Zhong G, Hogarth C, Huang W, Topping T, LaFrance J, *et al*. Knockout of Cyp26a1 and Cyp26b1 during postnatal life causes reduced lifespan, dermatitis, splenomegaly, and systemic inflammation in mice. FASEB Journal. 2020; 34: 15788–15804. https://doi.org/10.1096/fj.202001734R.

[41] Xu S, Yang G, Xu F, Yang Y, Wang J. Identification of prognostic biomarkers related to retinoic acid metabolism in gliomas and analysis of their impact on the immune microenvironment. Medicine. 2024; 103: e39836. https://doi.org/10.1097/MD.0000000000039836.

[42] di Masi A, Leboffe L, De Marinis E, Pagano F, Cicconi L, Rochette-Egly C, *et al*. Retinoic acid receptors: from molecular mechanisms to cancer therapy. Molecular Aspects of Medicine. 2015; 41: 1–115. https://doi.org/10.1016/j.mam.2014.12.003.

[43] Zolfaghari R, Mattie FJ, Wei CH, Chisholm DR, Whiting A, Ross AC. Using the human CYP26A1 gene promoter as a suitable tool for the determination of RAR-mediated retinoid activity. Methods in Enzymology. 2020; 637: 561–590. https://doi.org/10.1016/bs.mie.2020.03.013.

[44] Roberts C. Regulating Retinoic Acid Availability during Development and Regeneration: The Role of the CYP26 Enzymes. Journal of Developmental Biology. 2020; 8: 6. https://doi.org/10.3390/jdb8010006.

[45] Fenaux P, Degos L. Differentiation therapy for acute promyelocytic leukemia. The New England Journal of Medicine. 1997; 337: 1076–1077. https://doi.org/10.1056/NEJM199710093371509.

[46] Ge W, Song S, Qi X, Chen F, Che X, Sun Y, *et al*. Review and prospect of immune checkpoint blockade therapy represented by PD-1/PD-L1 in the treatment of clear cell renal cell carcinoma. Oncology Research. 2023; 31: 255–270. https://doi.org/10.32604/or.2023.027942.

[47] Nucera C, Lawler J, Parangi S. BRAF(V600E) and microenvironment in thyroid cancer: a functional link to drive can-

cer progression. Cancer Research. 2011; 71: 2417–2422. https://doi.org/10.1158/0008-5472.CAN-10-3844.

[48] Li Z, Lin Y, Cheng B, Zhang Q, Cai Y. Identification and Analysis of Potential Key Genes Associated With Hepatocellular Carcinoma Based on Integrated Bioinformatics Methods. Frontiers in Genetics. 2021; 12: 571231. https://doi.org/10.3389/fgene.2021.571231.

[49] Wang Y, Wang J, Yan K, Lin J, Zheng Z, Bi J. Identification of core genes associated with prostate cancer progression and outcome via bioinformatics analysis in multiple databases. PeerJ. 2020; 8: e8786. https://doi.org/10.7717/peerj.8786.

[50] Sneha S, Baker SC, Green A, Storr S, Aiyappa R, Martin S, *et al*. Intratumoural Cytochrome P450 Expression in Breast Cancer: Impact on Standard of Care Treatment and New Efforts to Develop Tumour-Selective Therapies. Biomedicines. 2021; 9: 290. https://doi.org/10.3390/biomedicines9030290.

[51] Wolbach SB, Howe PR. TISSUE CHANGES FOLLOWING DEPRIVATION OF FAT-SOLUBLE A VITAMIN. The Journal of Experimental Medicine. 1925; 42: 753–777. https://doi.org/10.1084/jem.42.6.753.

[52] Mi K, Zeng L, Chen Y, Yang S. Integrative Analysis of Single-Cell and Bulk RNA Sequencing Reveals Prognostic Characteristics of Macrophage Polarization-Related Genes in Lung Adenocarcinoma. International Journal of General Medicine. 2023; 16: 5031–5050. https://doi.org/10.2147/IJGM.S430408.

[53] Kandalaft LE, Motz GT, Duraiswamy J, Coukos G. Tumor immune surveillance and ovarian cancer: lessons on immune mediated tumor rejection or tolerance. Cancer Metastasis Reviews. 2011; 30: 141–151. https://doi.org/10.1007/s10555-011-9289-9.

[54] Zhang X, Liang Y. Decreased Expression of CPEB3 Predicts a Poor Prognosis in Patients with Melanoma: A Study Based on TCGA Data. BioMed Research International. 2021; 2021: 8197936. https://doi.org/10.1155/2021/8197936.

[55] Ma J, Jin J, Lu H, Zhang J, Li Y, Cai X. Exonuclease 1 is a Potential Diagnostic and Prognostic Biomarker in Hepatocellular Carcinoma. Frontiers in Molecular Biosciences. 2022; 9: 889414. https://doi.org/10.3389/fmolb.2022.889414.

[56] Vorobyeva DA, Potashnikova DM, Maryukhnich EV, Rusakovich GI, Tvorogova AV, Kalinskaya AI, *et al*. Cytokine production in an *ex vivo* model of SARS-CoV-2 lung infection. Frontiers in Immunology. 2024; 15: 1448515. https://doi.org/10.3389/fimmu.2024.1448515.

[57] Qu X, Tang Y, Hua S. Immunological Approaches Towards Cancer and Inflammation: A Cross Talk. Frontiers in Immunology. 2018; 9: 563.https://doi.org/10.3389/fimmu.2018.00563.

[58] Ding M, Wu G, Zhang S, Xie R, Yuan J, Xiao G, *et al*. Clinical Implications and Application of Molecular Testing in the Diagnosis and Management of Thyroid Nodules in the Chinese Population. Clinical Cancer Research. 2025; 31: 4996–5005. https://doi.org/10.1158/1078-0432.CCR-25-0270.

[59] Johnson WE, Li C, Rabinovic A. Adjusting batch effects in microarray expression data using empirical Bayes methods. Biostatistics. 2007; 8: 118–127. https://doi.org/10.1093/biostatistics/kxj037.